

RECEIVED: October 20, 2015

REVISED: December 3, 2015

ACCEPTED: December 19, 2015

PUBLISHED: January 5, 2016

Limits on neutrinophilic two-Higgs-doublet models from flavor physics

Enrico Bertuzzo,^a Yuber F. Perez G.,^a Olcyr Sumensari^{a,b} and Renata Zukanovich Funchal^a

^a*Departamento de Física Matemática, Instituto de Física, Universidade de São Paulo, C.P. 66.318, 05315-970 São Paulo, Brazil*

^b*Laboratoire de Physique Théorique (Bât. 210), CNRS (UMR 8627), Université Paris-Sud, Université Paris-Saclay, 91405 Orsay, France*

E-mail: bertuzzo@if.usp.br, yfperezg@if.usp.br, olcyr.sumensari@usp.br, zukanov@if.usp.br

ABSTRACT: We derive stringent limits on neutrinophilic two-Higgs-doublet models from low-energy observables after the discovery of the Higgs boson and of the mixing angle θ_{13} . These decays can constrain the plane spanned by m_{H^\pm} , the mass of the new charged Higgs, and v_2 , the vacuum expectation value of the new neutrinophilic scalar doublet. Lepton flavor conserving decays are not able to set meaningful bounds, since they depend strongly on the unknown neutrino absolute mass scale. On the other hand, loop induced lepton flavor violating decays, such as $\mu \rightarrow e\gamma$, $\mu \rightarrow 3e$ or $\mu \rightarrow e$ in nuclei are currently responsible for the best limits today. If $v_2 \lesssim 1$ (0.1) eV we get $m_{H^\pm} \gtrsim 250$ (2500) GeV at 90% CL. In the foreseen future these limits can improve by at least a factor of 100.

KEYWORDS: Beyond Standard Model, Neutrino Physics, Higgs Physics, Rare Decays

ARXIV EPRINT: [1510.04284](https://arxiv.org/abs/1510.04284)

Contents

1	Introduction	1
2	A brief description of the model	2
3	Experimental constraints from charged lepton processes	3
3.1	Lepton flavor conserving decays	4
3.2	Lepton flavor violating decays	5
3.2.1	$l_\alpha \rightarrow l_\beta \gamma$	5
3.2.2	$l_\alpha \rightarrow 3 l_\beta$	5
3.2.3	$\mu \rightarrow e$ in nuclei	7
3.2.4	$Z \rightarrow l_\alpha l_\beta$	8
3.2.5	$h \rightarrow l_\alpha l_\beta$	10
4	Conclusions	11
A	Limits from big bang nucleosynthesis	12

1 Introduction

The discovery of neutrino oscillations leaves basically no doubts on the fact that neutrinos are massive particles. Still, whether neutrinos are Dirac or Majorana particles is an open question. On a general ground, new physics in the neutral and charged lepton sectors are expected to be connected.

As it is well known, the easiest way to generate neutrino masses is via the addition of at least two right-handed (RH) neutrinos to the Standard Model (SM) particle content, with a Yukawa interaction $\mathcal{L} \supset H \bar{\ell}_L Y_\nu \nu_R$. Since the ν_R are necessarily gauge singlets, no gauge symmetry can forbid a Majorana mass term $\mathcal{L} \supset M_R \nu_R \nu_R$. Light neutrinos are a natural outcome in a seesaw scenario [1–4], where M_R is assumed to be very large. Once the RH neutrinos are integrated out, the Weinberg operator $(\ell H)^2/\Lambda$ is generated [5], producing Majorana neutrinos. In addition, heavy RH neutrinos may also generate the right amount of matter-antimatter asymmetry through leptogenesis [6].

On the contrary, if we insist on light RH neutrinos (i.e. small M_R), small neutrino masses require $Y_\nu \sim 10^{-(12 \div 13)}$, roughly 7 orders of magnitude smaller than the electron Yukawa coupling. Moreover, the presence of the RH Majorana mass makes the neutrinos pseudo-Dirac particles, rather than Dirac. In this case, baryogenesis is still possible through neutrino genesis [7], but the stringent cosmological limits on the number of relativistic degrees of freedom (RDOF) obtained by Planck [8] are a potential shortcoming. The

easiest way out is to impose the light ν_R to not contribute at all to the RDOF, i.e. to decouple from the plasma well before Big Bang Nucleosynthesis.

The tiny Yukawa couplings in the pseudo-Dirac case are of course a possibility, as they may find an explanation in a theory of flavor (just like any theory of flavor would explain the 5 orders of magnitude difference between the top and the electron Yukawa couplings). However, to get pure Dirac states, an additional symmetry must be imposed to forbid the RH Majorana mass. To avoid charging also some SM state under the same symmetry, this is most easily realized decoupling neutrino masses from the SM Higgs doublet. A second scalar, charged under the additional symmetry, can thus be introduced, whose vacuum expectation value (vev) is responsible for neutrino masses [9]. If the vev happens to be in the eV range, we obtain the correct order of magnitude for the neutrino masses with $\mathcal{O}(1)$ Yukawa couplings. Models with such a *neutrinophilic* doublet and pure Dirac neutrinos were studied in some detail in [10]. Recently, after the discovery of the Higgs boson by the LHC experiments, these minimal Neutrinophilic Two-Higgs-Doublet Models (ν 2HDM) were revisited and strong bounds were imposed on their scalar spectrum [11].

We focus here on additional experimental consequences from charged lepton flavor physics on ν 2HDM, in particular, after the last neutrino mixing angle, θ_{13} , was precisely measured by the reactor experiments Daya Bay [12] and Double Chooz [13]. Note that non-standard interactions in the neutrino sector only involve RH neutrinos in these models, so they are not expected to affect neutrino oscillations.

In section 2 we describe the main features of ν 2HDM that are important to understand how they modify lepton flavor physics. In section 3 we calculate the most constraining processes involving charged leptons that are affected by ν 2HDM: tree-level flavor conserving leptonic decays, loop induced flavor violating leptonic decays, tree-level flavor violating Z and Higgs decays. We derive current bounds on the model parameters by using the most precise experimental data available today and estimate the improved sensitivity of future experiments to these parameters. In section 4 we present our final conclusions.

2 A brief description of the model

Let us now describe the class of models we are interested in. We extend the SM particle content to include a second Higgs doublet H_2 , as well as three RH neutrinos ν_R . H_2 has the same gauge quantum numbers as the ordinary Higgs H_1 , while the RH neutrinos ν_R are gauge singlets. The interactions we are interested in are given by

$$-\mathcal{L}_{\text{Yuk}} = \bar{e}_R Y_E H_1 \ell_L + \bar{\nu}_R Y_N \tilde{H}_2 \ell_L + \text{h.c.}, \quad (2.1)$$

where $\tilde{H}_2 = i\sigma_2 H_2^*$ is the conjugate of H_2 . The previous lagrangian can be easily obtained requiring H_2 and ν_R^i to have the same charge under an additional global $U(1)_X$ [10], or imposing a \mathbb{Z}_2 symmetry [9]. In the following we will not be concerned with the specific realization from which eq. (2.1) is obtained, focusing only on its consequences on flavor processes.

Using the PMSN matrix U to express the gauge eigenstates ν_α in terms of the mass eigenstates ν_i , $\nu_\alpha = U_{\alpha i} \nu_i$, from eq. (2.1) we get

$$-\mathcal{L}_{\text{Yuk}} = H_1^0 \bar{e} \hat{Y}_E P_L e + H_2^0 \bar{\nu}_i \hat{Y}_N^i P_L \nu_i - H_2^+ \bar{\nu}_i (\hat{Y}_N U^\dagger)_{i\beta} P_L e_\beta + \text{h.c.}, \quad (2.2)$$

where $\hat{Y}_{E,N}$ are diagonal matrices of Yukawa couplings. Assuming H_2 to acquire a vev $v_2 \lesssim \mathcal{O}(\text{eV}) \ll v_1 \simeq 246 \text{ GeV}$, we get that $\mathcal{O}(1)$ Yukawa couplings in the neutrino sector are possible. Moreover, since $v_2 \ll v_1$, we can identify H_1 with the SM Higgs doublet, while the second doublet can be written in terms of the additional scalar mass eigenstates, H , A and H^+ , as $H_2 \simeq (-H^+, \frac{H+iA}{\sqrt{2}})^T$. Let us stress that if an exact $U(1)_X$ symmetry is present also in the scalar potential, A is a strictly massless Goldstone boson. This calls for an explicit symmetry breaking to make the model phenomenologically viable, which in [10] is given by a soft term in the potential.¹

Given its importance for the following sections, let us rewrite the coupling involving the charged Higgs in the neutrino flavor basis:

$$-\mathcal{L}_{\text{charged}} = \sqrt{2} \frac{U_{\alpha i} m_{\nu_i} U_{\beta i}^*}{v_2} H_2^+ \bar{\nu}_\alpha P_L e_\beta + \text{h.c.}, \quad \alpha, \beta = e, \mu, \tau. \quad (2.3)$$

It is clear that apart from the v_2 dependence, the coupling is completely fixed in terms of (known) neutrino parameters. Integrating out the massive charged Higgs boson, we obtain

$$-\mathcal{L}_{\text{eff}} = \frac{1}{m_{H^\pm}^2} \frac{\langle m_{\alpha\beta} \rangle}{v_2} \frac{\langle m_{\rho\sigma} \rangle}{v_2} (\bar{\nu}_\alpha \gamma^\mu P_R \nu_\sigma) (\bar{e}_\rho \gamma_\mu P_L e_\beta) + \dots, \quad (2.4)$$

where $\langle m_{\alpha\beta} \rangle = U_{\alpha i} m_{\nu_i} U_{\beta i}^*$ and only the non-standard neutrino interaction term is displayed. As already anticipated in the introduction, this term only involves RH neutrinos. Since eq. (2.4) does not have an analog term in the quark sector, we do not expect RH neutrinos to be produced at a relevant rate by nuclear processes, for instance, in the sun, in such a way that there is no modification of neutrinos propagation through matter.

3 Experimental constraints from charged lepton processes

The phenomenology of a neutrinophilic charged Higgs in low-energy processes is different from the one of a generic 2HDM, mainly because the couplings with leptons are highly enhanced by a factor $v_1/v_2 \gg 1$, while the couplings with quarks are highly suppressed by $v_2/v_1 \ll 1$. As a first consequence, the ν 2HDM easily evades the limits coming from hadronic observables such as $B \rightarrow X_s \gamma$, mesons mixing and, more importantly, leptonic and semi-leptonic B meson decays [15–17]. On the other hand, leptonic observables (normally suppressed by neutrino masses) may now receive sizable contributions, as we are now going to show. Our main results are summarized in figure 4, where we show the current bounds (left panel) and the expected future sensitivities (right panel) on the (m_{H^\pm}, v_2) plane.

¹A massless neutrinophilic scalar would be in conflict with several constraints, such as stellar cooling [14] and electroweak precision tests [11]. In addition, compatibility with the total number of relativistic degrees of freedom measured by Planck [8] would impose very strong constraints on its parameter space (see appendix A).

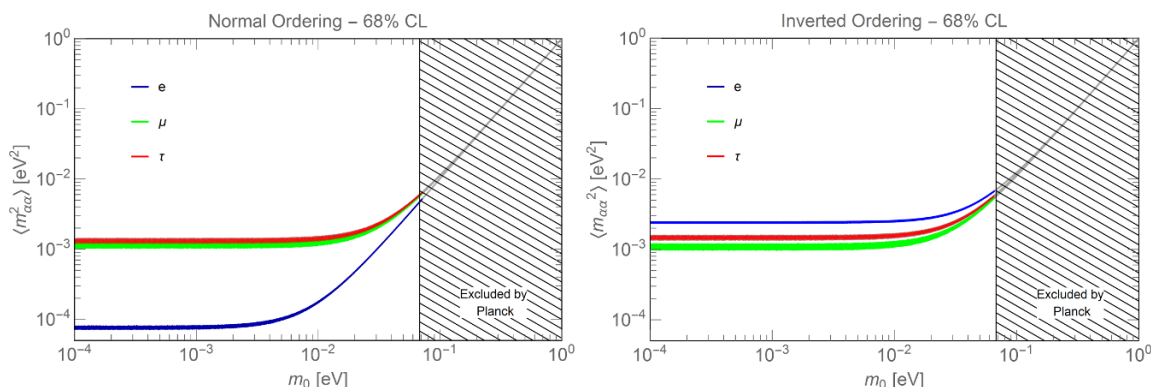


Figure 1. Values of $\langle m_{\alpha\alpha}^2 \rangle$ as a function of the lightest neutrino mass m_0 obtained scanning over the 1σ range of the oscillation parameters [18]. Blue region: $\alpha = e$, green region: $\alpha = \mu$, red region: $\alpha = \tau$. The left panel refers to the Normal neutrino mass ordering (NO), the right panel to the Inverted ordering (IO). The gray points are excluded by Planck’s limit on the sum of neutrinos masses [8, 19].

3.1 Lepton flavor conserving decays

Let us look at the tree level μ and τ leptonic decays. The charged scalar contribution to $\ell_\alpha \rightarrow \ell_\beta \bar{\nu} \nu$ induces a violation of lepton flavor universality (LFU), which can be effectively encoded in the definition of “flavorful” gauge couplings g_α [20]. Experimentally, they can be measured from the τ and μ lifetimes. The total decay width for $\ell_\alpha \rightarrow \ell_\beta \bar{\nu} \nu$ in the presence of a charged Higgs boson can be written as $\Gamma(\ell_\alpha \rightarrow \ell_\beta \bar{\nu} \nu) = \Gamma^{\text{SM}}(\ell_\alpha \rightarrow \ell_\beta \bar{\nu} \nu)(1 + \langle m_{\alpha\alpha}^2 \rangle \langle m_{\beta\beta}^2 \rangle \rho^2 / 8)$ [10, 21], from which

$$\begin{aligned} \left(\frac{g_\mu}{g_e}\right)^2 &\simeq 1 + \frac{\langle m_{\tau\tau}^2 \rangle (\langle m_{\mu\mu}^2 \rangle - \langle m_{ee}^2 \rangle)}{8} \rho^2, \\ \left(\frac{g_\mu}{g_\tau}\right)^2 &\simeq 1 + \frac{\langle m_{ee}^2 \rangle (\langle m_{\mu\mu}^2 \rangle - \langle m_{\tau\tau}^2 \rangle)}{8} \rho^2. \end{aligned} \tag{3.1}$$

We have defined $\langle m_{\alpha\beta}^2 \rangle = U_{\alpha i} m_{\nu_i}^2 U_{\beta i}^*$ and $\rho = (G_F m_{H^\pm}^2 v_2^2)^{-1}$.

Although from eq. (3.1) it may look like it is possible to use the experimental results on g_μ/g_e and g_μ/g_τ to extract bounds on ρ , we stress that (i) the experimental data are well compatible with lepton flavor universality at 1σ ,² and (ii) although the differences $\langle m_{\alpha\alpha}^2 \rangle - \langle m_{\beta\beta}^2 \rangle$ are independent of the value of the lightest neutrino mass m_0 , the individual values of $\langle m_{ee}^2 \rangle$ and $\langle m_{\tau\tau}^2 \rangle$ depend crucially on m_0 , as shown in figure 1. From this plot, it is clear that the flavorful couplings reach very small values for $m_0^2 \ll \Delta m_{ij}^2$, making them always compatible with the current bounds on LFU [20]. Since the absolute neutrino mass scale is still unknown, no information can be extracted from these observables.

²We are aware of the 2σ disagreement between the PDG and HFAG fits of $B_\mu = \text{BR}(\tau \rightarrow \mu \nu_\tau \bar{\nu}_\mu)$ with respect to the SM [22, 23]. However, we notice that the world average of B_μ , which we are considering here, is in perfect agreement with the SM prediction. The main difference between these two results is the inclusion of the ratio B_μ/B_e measured precisely by BaBar, which has a slight disagreement of 1.6σ with the leptonic universality assumption [24].

3.2 Lepton flavor violating decays

We will study here loop induced lepton flavor violating (LFV) processes that can currently, or in the near future, be constrained by data, and the corresponding consequences on the allowed values of the ν 2HDM parameters.

3.2.1 $\ell_\alpha \rightarrow \ell_\beta \gamma$

Let us start with loop induced processes, for which strong experimental constraints are available, at least in the $\mu \rightarrow e \gamma$ channel. For a generic process $\ell_\alpha \rightarrow \ell_\beta \gamma$, the scalar mediated branching ratio reads [21]

$$\text{BR}(\ell_\alpha \rightarrow \ell_\beta \gamma) = \text{BR}(\ell_\alpha \rightarrow e \bar{\nu} \nu) \frac{\alpha_{\text{EM}}}{192\pi} |\langle m_{\alpha\beta}^2 \rangle|^2 \rho^2. \quad (3.2)$$

The strongest experimental bound on this type of process comes from the MEG-2 upper limit $\text{BR}(\mu \rightarrow e \gamma) < 5.7 \times 10^{-13}$ [25], while weaker bounds on the other channels are obtained by the BaBar Collaboration, $\text{BR}(\tau \rightarrow e \gamma) < 3.3 \times 10^{-8}$ and $\text{BR}(\tau \rightarrow \mu \gamma) < 4.4 \times 10^{-8}$ [26]. In terms of ρ (defined below eq. (3.1)), we get the 90% C.L. bounds³

$$\begin{aligned} \rho &\lesssim 1.2 \text{ eV}^{-2} & [\mu \rightarrow e \gamma], \\ \rho &\lesssim 730 \text{ eV}^{-2} & [\tau \rightarrow e \gamma], \\ \rho &\lesssim 793 \text{ eV}^{-2} & [\tau \rightarrow \mu \gamma]. \end{aligned} \quad (3.3)$$

This is the best limit at present on the parameters v_2 and m_{H^\pm} , and it already implies that, insisting on $v_2 \lesssim 1 \text{ eV}$, we must have $m_{H^\pm} \gtrsim 250 \text{ GeV}$. With the future improvement on the MEG expected sensitivity, $\text{BR}(\mu \rightarrow e \gamma) \sim 5 \times 10^{-14}$ [27, 28], the corresponding bound on ρ can be improved by about one order of magnitude to $\rho \lesssim 0.4 \text{ eV}^{-2}$. The limits imposed by the MEG bound on the (m_{H^\pm}, v_2) plane are shown in figure 4, blue line, for the current result (left panel), as well as for the expected future sensitivity (right panel).

We would like to point out that in case a positive sign of $\mu \rightarrow e \gamma$ is observed in the near future, ν 2HDM predicts a relation between $\text{BR}(\mu \rightarrow e \gamma)$ and $\text{BR}(\tau \rightarrow e \gamma, \mu \gamma)$ which is actually sensitive to δ_{CP} . We show in figure 2 the ratio of these branching ratios as a function of δ_{CP} . Although it is very unlikely to be able to experimentally probe $\text{BR}(\tau \rightarrow e \gamma, \mu \gamma)$ down to 10^{-14} in the near future, from figure 2 we see that a limit on $\text{BR}(\mu \rightarrow e \gamma)$ would also set a stringent limit on $\text{BR}(\tau \rightarrow e \gamma, \mu \gamma)$ independently of δ_{CP} . Moreover, if δ_{CP} can be measured by neutrino oscillations experiments, this result can be translated into a correlation of the different LFV branching ratios.

3.2.2 $\ell_\alpha \rightarrow 3 \ell_\beta$

We now turn our attention to processes involving three charged leptons in the final state. These processes can be described by the loop induced effective lagrangian

$$\mathcal{L}_{\text{eff}} = \frac{e m_\alpha}{2} A_D \bar{\ell}_\beta \sigma_{\mu\nu} \ell_\alpha F^{\mu\nu} + e A_{ND} \bar{\ell}_\beta \gamma_\mu P_L \ell_\alpha A^\mu + e^2 B (\bar{\ell}_\alpha \gamma_\mu P_L \ell_\beta) (\bar{\ell}_\beta \gamma_\mu P_L \ell_\beta) + \text{h.c.}, \quad (3.4)$$

³These limits have a very loose dependence on the neutrino mass hierarchy. Here, we always present the most pessimistic bound, which for $\mu \rightarrow e \gamma$ and $\tau \rightarrow \mu \gamma$ is obtained in the NO, while for $\tau \rightarrow e \gamma$ the IO is slightly less constraining.

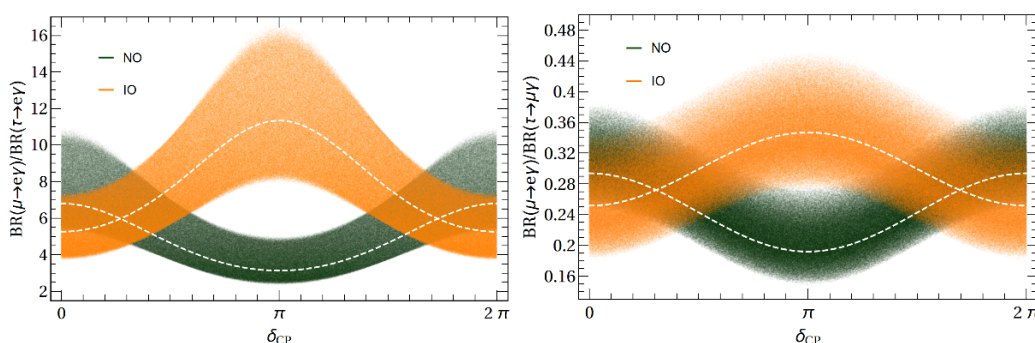


Figure 2. Ratios $\text{BR}(\mu \rightarrow e\gamma)/\text{BR}(\tau \rightarrow e\gamma)$ (right panel) and $\text{BR}(\mu \rightarrow e\gamma)/\text{BR}(\tau \rightarrow \mu\gamma)$ (left panel) as a function of δ_{CP} . The bands were obtained by scanning over the 2σ range of the oscillation parameters with respect to the central values (white dashed lines), which correspond to the best fit [18].

where m_α is the mass of the charged lepton in the initial state, and $A_{(N)D}$ and B are Wilson coefficients associated to γ -penguin diagrams and charged Higgs boxes, respectively. Neglecting neutrino masses and imposing $m_\beta/m_\alpha \ll 1$, we derived the following expressions,

$$A_D = \frac{1}{6(4\pi)^2} \frac{1}{m_{H^\pm}^2} \frac{\langle m_{\alpha\beta}^2 \rangle}{v_2^2}, \quad (3.5)$$

$$A_{ND} = \frac{1}{9(4\pi)^2} \frac{q^2}{m_{H^\pm}^2} \frac{\langle m_{\alpha\beta}^2 \rangle}{v_2^2}, \quad (3.6)$$

$$e^2 B = -\frac{2}{(4\pi)^2} \frac{\langle m_{\alpha\beta}^2 \rangle \langle m_{\beta\beta}^2 \rangle}{m_{H^\pm}^2 v_2^4}, \quad (3.7)$$

where q^2 is the photon squared momentum in the penguin-like diagrams.⁴ We neglect the Z -penguin diagrams, since they are suppressed by m_β and by the Z boson mass.

Our results for the Wilson coefficients are in full agreement with those of ref. [29], where the impact of the scotogenic model on $\mu \rightarrow 3e$ was studied. Although these models are intrinsically different, one can retrieve the $\nu 2\text{HDM}$ loop functions by replacing the mass of RH neutrinos by the active ones and by matching the Yukawa lagrangians of the two models. The only difference between the two calculations is a new Z -penguin diagram with two neutrinos in the loop, which is only present in the $\nu 2\text{HDM}$ model (see figure 3). This diagram does not exist in the scotogenic model, because the \mathbb{Z}_2 symmetry forbids the mixing between the active and sterile neutrinos. However, this diagram is additionally suppressed by the active neutrino mass, giving a negligible contribution.

In terms of the coefficients defined above, the branching ratio reads

$$\begin{aligned} \text{BR}(\ell_\alpha \rightarrow \ell_\beta \ell_\beta \ell_\beta) = \text{BR}(\ell_\alpha \rightarrow e\bar{\nu}\nu) \frac{3(4\pi)^2 \alpha_{\text{EM}}^2}{8 G_F^2} \left[\frac{|A_{ND}|^2}{q^4} + |A_D|^2 \left(\frac{16}{3} \log \left(\frac{m_\alpha}{m_\beta} \right) - \frac{22}{3} \right) \right. \\ \left. + \frac{1}{6} |B|^2 + 2 \text{Re} \left(-2 \frac{A_{ND}}{q^2} A_D^* + \frac{1}{3} \frac{A_{ND}}{q^2} B^* - \frac{2}{3} A_D B^* \right) \right], \quad (3.8) \end{aligned}$$

⁴Notice that the dimension four contribution vanishes for off-shell photons, as required by gauge invariance.

$\frac{A}{Z}$ Nucleus	Z_{eff}	F_p	Γ_{capt} (GeV)
${}_{13}^{27}\text{Al}$	11.5	0.64	4.64079×10^{-19}
${}_{22}^{48}\text{Ti}$	17.6	0.54	1.70422×10^{-18}
${}_{79}^{197}\text{Au}$	33.5	0.16	8.59868×10^{-18}

Table 1. Nuclear parameters used in our analysis, taken from [32].

where the sub-leading terms in m_β/m_α have been neglected. Notice that the box terms have a different dependence on v_2 and therefore this expression cannot be expressed only in terms of ρ . Moreover, from eqs. (3.5)–(3.7) it is clear that the box contribution dominates for small values of v_2 .

For relatively large values of v_2 , in the region where the penguin diagrams dominate, we can use the current experimental limit, $\text{BR}(\mu \rightarrow e^-e^-e^+) < 1 \times 10^{-12}$ [30] to directly put the bound $\rho \lesssim 22 \text{eV}^{-2}$. This is not possible for small v_2 , in the region where the box dominates, since the corresponding Wilson coefficient cannot be expressed in terms of ρ . The total bound is shown in figure 4, green line. The current experimental limit (left panel), is stronger than the limit derived from $\mu \rightarrow e\gamma$ for $v_2 \lesssim 0.01 \text{eV}$. The situation will change with the future Mu3e experiment, which aims to reach an ultimate sensitivity of $\text{BR}(\mu \rightarrow e^-e^-e^+) \sim 1 \times 10^{-16}$ [31]. As can be seen from figure 4, right panel, the future sensitivity on $\mu \rightarrow 3e$ is expected to be stronger than the one from $\mu \rightarrow e\gamma$.

3.2.3 $\mu \rightarrow e$ in nuclei

The $\mu - e$ conversion in nuclei is another LFV process that appears in $\nu 2\text{HDM}$. It is important to note that the experimental collaborations have announced great future sensitivities, making this a relevant bound for different neutrino mass models. In our framework, the dominant contributions are only the γ -penguins, since the Z -penguins are suppressed by the electron and Z boson masses, while box diagrams and scalar penguins are suppressed by the tiny coupling of the neutrinophilic scalars with quarks. Keeping only the dominant contributions, the conversion rate is given by [29, 32, 33]

$$\text{CR}(\mu - e, \text{nucleus}) = \frac{p_e E_e m_\mu^3 G_F^2 \alpha_{\text{EM}}^3 Z_{\text{eff}}^4 F_p^2}{8\pi^2 Z \Gamma_{\text{capt}}} \left| (Z + N)g_{LV}^{(0)} + (Z - N)g_{LV}^{(1)} \right|^2, \quad (3.9)$$

where $p_e, E_e \approx m_\mu$ are the electron momentum and energy, respectively, which are approximately equal to the muon mass; Z, N are the number of protons and neutrons in the nucleus, Z_{eff} is the effective atomic charge and F_p is the nuclear matrix element, given in table 1 for the nuclei we are considering in our study. Notice that the conversion rate is normalized to the muon capture rate Γ_{capt} . The coefficients $g_{LV}^{(0,1)}$ are given by [32, 33]

$$g_{LV}^{(0)} = \frac{1}{2} \sum_{q=u,d} \left(G_V^{(q,p)} g_{LVq} + G_V^{(q,n)} g_{LVq} \right), \quad (3.10a)$$

$$g_{LV}^{(1)} = \frac{1}{2} \sum_{q=u,d} \left(G_V^{(q,p)} g_{LVq} - G_V^{(q,n)} g_{LVq} \right). \quad (3.10b)$$

Nucleus	Present Bound	Future Sensitivity
Al	–	$10^{-15} - 10^{-18}$ [34]
Ti	4.3×10^{-12} [35]	$\sim 10^{-18}$ [36]
Au	7×10^{-13} [37]	–

Table 2. Present bound and future sensitivity on the $\mu - e$ nuclear conversion rate [38].

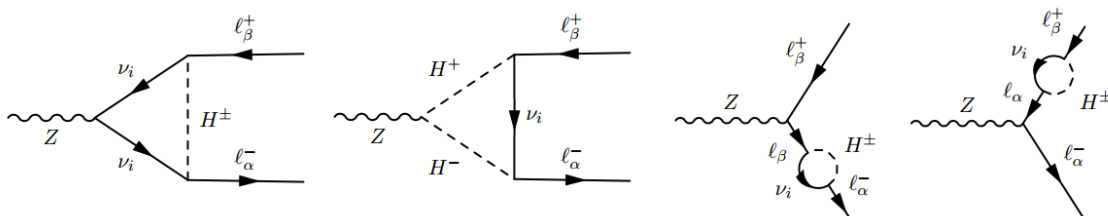


Figure 3. Penguin and self-energy diagrams contributing to the Z LFV decays.

We stress that we consider only vector couplings, since only the γ -penguins are relevant for this process. Also, we should note that only valence quarks will be relevant for our purpose, because the sea quarks, like the strange quark, interact effectively only through the scalar part [32]. The coupling g_{LVq} is given by

$$g_{LVq} = \frac{\sqrt{2}}{G_F} e^2 Q_q \left(\frac{A_{ND}}{q^2} - A_D \right). \tag{3.11}$$

where Q_q is the quark charge. For completeness, we quote here the values of the coefficients $G_V^{(q,p)}$ [32]:

$$G_V^{(u,p)} = G_V^{(d,n)} = 2, \quad G_V^{(u,n)} = G_V^{(d,p)} = 1. \tag{3.12}$$

From the present bounds on the $\mu - e$ conversion rate, table 2, we get $\rho \lesssim 30 \text{ eV}^{-2}$ for titanium (Ti), and $\rho \lesssim 13.5 \text{ eV}^{-2}$ for gold (Au), while from the future expected sensitivities in aluminium (Al) and titanium we get $\rho \lesssim 0.020 \text{ eV}^{-2}$ and $\rho \lesssim 0.015 \text{ eV}^{-2}$, respectively. We stress that $\mu - e$ conversion in nuclei will be, in the future, the most sensitive process to probe ν 2HDM, if the experiments reach the announced sensitivities. In figure 4 we see how $\mu - e$ conversion sets limits on the (m_{H^\pm}, v_2) plane using the present results (left panel) and the forecast sensitivity (right panel).

3.2.4 $Z \rightarrow \ell_\alpha \ell_\beta$

Besides their impact on charged lepton decays, neutrinophilic scalars can give rise to LFV Z boson decays. In our framework, the additional one-loop diagrams contributing to this process are shown in figure 3, where ℓ_α and ℓ_β are charged leptons of different flavors. The effective Hamiltonian can be written as

$$\mathcal{H}_{\text{eff}} = C_V \bar{\ell}_\alpha \gamma^\mu P_L \ell_\beta Z_\mu + \text{h.c.} \tag{3.13}$$

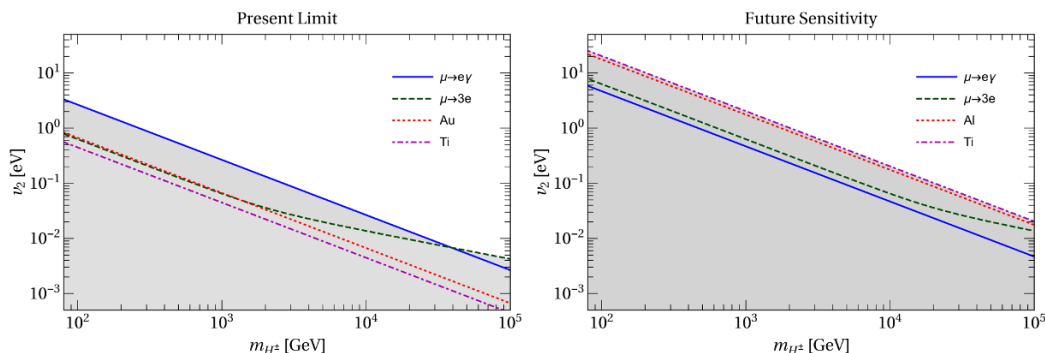


Figure 4. On the left panel we show the current limits on (m_{H^\pm}, v_2) plane coming from $\mu \rightarrow e\gamma$, $\mu \rightarrow eee$ and $\mu \rightarrow e$ in nuclei. The regions below these lines are excluded at 90% CL. On the right panel we show the predicted sensitivities of future experiments. The parameter region above each of these lines can be explored by the respective experiment.

Neglecting fermion masses, the Wilson coefficient C_V is given by

$$C_V = \frac{1}{64\pi^2} \frac{g \cos(2\theta_W)}{\cos \theta_W} \frac{\langle m_{\alpha\beta}^2 \rangle}{v_2^2} \left\{ 4 \left(\frac{2}{x_Z} - 1 \right) \left(\frac{4}{x_Z} - 1 \right)^{1/2} \arctan \left[\left(\frac{4}{x_Z} - 1 \right)^{-1/2} \right] - \frac{16}{x_Z^2} \arctan^2 \left[\left(\frac{4}{x_Z} - 1 \right)^{-1/2} \right] + \left(5 - \frac{4}{x_Z} \right) \right\}, \quad (3.14)$$

with $x_Z = m_Z^2/m_{H^\pm}^2 < 1$. In the $x_Z \ll 1$ limit this expression can be further simplified to

$$C_V = \frac{x_Z}{288\pi^2} \frac{g \cos(2\theta_W)}{\cos \theta_W} \frac{\langle m_{\alpha\beta}^2 \rangle}{v_2^2} + \mathcal{O}(x_Z^2). \quad (3.15)$$

The Wilson coefficient C_V directly enters in the expression for the $Z \rightarrow \ell_\alpha \ell_\beta$ decay width, which in the limit of vanishing lepton masses is given by

$$\Gamma(Z \rightarrow \ell_\alpha^\pm \ell_\beta^\mp) = \frac{m_Z}{12\pi\Gamma_Z} |C_V|^2, \quad (3.16)$$

where m_Z and Γ_Z are the Z mass and total decay width and we took into account that $\Gamma(Z \rightarrow \ell_\alpha^\pm \ell_\beta^\mp) = \Gamma(Z \rightarrow \ell_\alpha^- \ell_\beta^+) + \Gamma(Z \rightarrow \ell_\alpha^+ \ell_\beta^-)$.

On the experimental side, the most constraining bound comes from the ATLAS upper limit $\text{BR}(Z \rightarrow e^\pm \mu^\mp) < 7.5 \times 10^{-7}$ [39]. The channels with a τ lepton in the final state were only studied at LEP and have weaker experimental limits, $\text{BR}(Z \rightarrow e^\pm \tau^\mp) < 9.8 \times 10^{-6}$ and $\text{BR}(Z \rightarrow \mu^\pm \tau^\mp) < 1.2 \times 10^{-5}$ [40].

Using ATLAS current limit on $Z \rightarrow e^\pm \mu^\mp$ we get an upper bound $\rho \lesssim 3.5 \times 10^3 \text{ eV}^{-2}$, much weaker than any of the bounds presented so far. Even considering the expected sensitivity at a future electron-positron collider operating at the Z pole (TLEP), $\text{BR}(Z \rightarrow e^\pm \mu^\mp) \sim 10^{-13}$ [38], the situation is not going to improve much. Instead, if we consider the current bounds on the parameter ρ coming from $\mu \rightarrow e\gamma$, then we can predict $\text{BR}(Z \rightarrow e^\pm \mu^\mp) \lesssim 10^{-17}$ and $\text{BR}(Z \rightarrow \mu^\pm \tau^\mp) \lesssim 10^{-16}$.

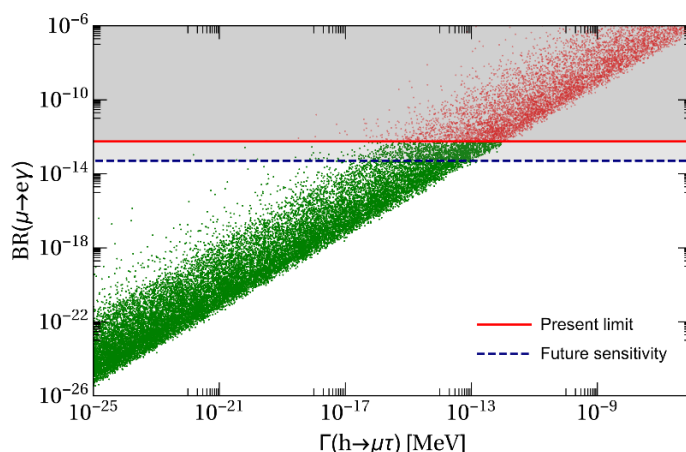


Figure 5. $\Gamma(h \rightarrow \mu\tau)$ as a function of $\text{BR}(\mu \rightarrow e\gamma)$ for the allowed parameter space of the $\nu 2\text{HDM}$ of ref. [10]. The gray regions correspond to the current exclusion by MEG-2 [25] (red line) and to the future expected sensitivity (blue, dashed line).

3.2.5 $h \rightarrow \ell_\alpha \ell_\beta$

In this section we briefly discuss the LFV process $h \rightarrow \ell_\alpha \ell_\beta$, where h denotes the SM-like Higgs. The effective Hamiltonian describing this decay can be written as

$$\mathcal{H}_{\text{eff}} = C_L \bar{\ell}_\alpha P_L \ell_\beta h + \text{h.c.} \quad (3.17)$$

Assuming $m_\beta/m_\alpha \ll 1$, the Wilson coefficient C_L reads

$$C_L = -\frac{1}{8\pi^2} \frac{\langle m_{\alpha\beta}^2 \rangle}{v_2^2} \frac{m_\alpha g_{hH^+H^-}}{m_{H^\pm}^2} \frac{1}{y_H} \left\{ 1 - 2 \left(\frac{4}{y_H} - 1 \right)^{1/2} \arctan \left[\left(\frac{4}{y_H} - 1 \right)^{-1/2} \right] \right. \quad (3.18)$$

$$\left. + \frac{4}{y_H} \arctan^2 \left[\left(\frac{4}{y_H} - 1 \right)^{-1/2} \right] \right\}, \quad (3.19)$$

with $y_H = m_h^2/m_{H^\pm}^2$. The coupling $g_{hH^+H^-}$ is defined as the trilinear coupling hH^+H^- and depends on the particular realization of the scalar sector. In the asymptotic limit,

$$C_L = -\frac{1}{32\pi^2} \frac{\langle m_{\alpha\beta}^2 \rangle}{v_2^2} \frac{m_\alpha g_{hH^+H^-}}{m_{H^\pm}^2} \left[1 + \frac{y_H}{9} + \mathcal{O}(y_H^2) \right]. \quad (3.20)$$

The decay rate $\Gamma(h \rightarrow \ell_\alpha^\pm \ell_\beta^\mp) = \Gamma(h \rightarrow \ell_\alpha^+ \ell_\beta^-) + \Gamma(h \rightarrow \ell_\alpha^- \ell_\beta^+)$ reads

$$\Gamma(h \rightarrow \ell_\alpha^\pm \ell_\beta^\mp) = \frac{(m_h^2 - m_\alpha^2)^2}{8\pi m_h^3} |C_L|^2. \quad (3.21)$$

In order to make predictions for LFV Higgs decays, one needs to consider a specific realization of the scalar potential and scan over the parameter space allowed by theoretical and phenomenological constraints. Here, we consider the model proposed in ref. [10] which, as discussed in [11] is the only minimal realization of the $\nu 2\text{HDM}$ still consistent with

electroweak precision measurements. Scanning over the allowed parameter space of this model (see [11] for details), we obtain a prediction for $\Gamma(h \rightarrow \mu\tau)$, the largest LFV Higgs decay, as a function of $\text{BR}(\mu \rightarrow e\gamma)$, as shown in figure 5. We see that due to the stringent limit imposed by MEG-2, $\Gamma(h \rightarrow \mu\tau)$ cannot exceed 10^{-9} MeV , so this model cannot possibly explain a branching ratio as high as $\text{BR}(H \rightarrow \mu\tau) = (0.84_{-0.37}^{+0.39}) \%$ as measured by CMS [41]. Unfortunately, such a small branching ratio is also completely out of the reach of the LHC or even of any foreseen future Higgs precision experiment.

4 Conclusions

We have focused our study on the neutrinophilic two-Higgs-doublets model scenario, $\nu 2\text{HDM}$, in which a neutrinophilic Higgs doublet is responsible for neutrino masses through a tiny vev $v_2 \lesssim 1 \text{ eV}$ and in which neutrinos are Dirac particles. Interestingly, in this scenario indirect limits are much more effective in constraining the parameter space than direct collider searches. This is due to the fact that the new scalars basically only couple to leptons and gauge bosons, in such a way that only the quite weak direct limit from LEP applies, $m_{H^\pm} \gtrsim 80 \text{ GeV}$ [42].

Indirect limits can come either from lepton flavor conserving or from lepton flavor changing processes. The important point is that such flavor effects are controlled by the effective neutrino mass $\langle m_{\alpha\beta}^2 \rangle$, defined below eq. (3.1), so that they can be well predicted now that, thanks to the measurement of the last mixing angle θ_{13} , we are entering in the era of precision neutrino physics. This allows to put stringent limits on two of the unknown parameters of the $\nu 2\text{HDM}$, namely the mass of the neutrinophilic charged Higgs boson, m_{H^\pm} , and the vev of the neutrinophilic doublet, v_2 . Let us stress that, although the neutrinophilic charged Higgs boson modifies the neutrino propagation in matter, this modification affects only the right-handed neutrinos, which are not produced with a relevant rate in the sun.

In this paper we have investigated limits coming from $\mu \rightarrow e\gamma$, $\tau \rightarrow \mu(e)\gamma$, $\mu \rightarrow 3e$, $\mu \rightarrow e$ in nuclei, lepton flavor violating Z and Higgs decays. Other limits, like the one coming from Big Bang Nucleosynthesis, turn out to be weaker (see appendix A). Our main results are summarized in figure 4. On the left panel we show the current bounds, which are dominated by $\mu \rightarrow e\gamma$ for $v_2 \gtrsim 0.01 \text{ eV}$ and by $\mu \rightarrow eee$ for $v_2 \lesssim 0.01 \text{ eV}$. For example, in the region dominated by $\mu \rightarrow e\gamma$, we get a lower bound of $m_{H^\pm} \gtrsim 250 (2500) \text{ GeV}$ for $v_2 \lesssim 1 (0.1) \text{ eV}$ at 90% CL, while in the region dominated by $\mu \rightarrow 3e$ the lower bound on the charged Higgs boson mass is worse than $(30 - 40) \text{ TeV}$. Since the philosophy of the $\nu 2\text{HDM}$ is to allow for $\mathcal{O}(1)$ Yukawa couplings in the neutrino sector, we do not expect the $v_2 \ll 0.01 \text{ eV}$ region to be particularly relevant. In the right panel of figure 4 we instead show the future sensitivity, in which the limits could be largely dominated by $\mu - e$ conversion in nuclei. In this case, if nothing is observed, we expect the lower bound for $v_2 = 1 \text{ eV}$ to get as stringent as $m_{H^\pm} \gtrsim 2 \text{ TeV}$, and the one for $v_2 = 0.1 \text{ eV}$ to become $m_{H^\pm} \gtrsim 20 \text{ TeV}$.

Let us conclude mentioning that this model predicts lepton flavor violating Higgs decays, which is an interesting possibility in light of the recently CMS observation of an excess in the $h \rightarrow \mu\tau$ channel [41]. Unfortunately, the region compatible with the observed value for the branching ratio is already excluded by the $\mu \rightarrow e\gamma$ limit, figure 5, in

such a way that such an excess cannot be observed in the ν 2HDM framework. Similarly, $\text{BR}(Z \rightarrow \ell_\alpha \ell_\beta)$, with $\ell_\alpha \neq \ell_\beta$, is constrained to be $\lesssim 10^{-16}$ by the experimental limit on $\mu \rightarrow e\gamma$, making this observable beyond the reach of the current experiments.

Acknowledgments

We thank Takashi Toma for useful correspondence. This work was supported by Fundação de Amparo à Pesquisa do Estado de São Paulo (FAPESP) and Conselho Nacional de Ciência e Tecnologia (CNPq). We also acknowledge partial support from the European Union FP7 ITN INVISIBLES (Marie Curie Actions, PITN-GA-2011-289442).

A Limits from big bang nucleosynthesis

Let us now discuss the limits on the ν 2HDM coming from Big Bang Nucleosynthesis. The standard definition for the number of relativistic degrees of freedom N_{eff} , and its expression in the ν 2HDM, are given by

$$\rho = N_{\text{eff}} \frac{7}{8} \left(\frac{4}{11} \right)^{4/3} \rho_\gamma, \quad N_{\text{eff}} = \left(\frac{11}{4} \right)^{4/3} 3 \left[\left(\frac{T_{\nu L}}{T_\gamma} \right)^4 + \left(\frac{T_{\nu R}}{T_\gamma} \right)^4 \right], \quad (\text{A.1})$$

to be compared with the result of the Planck collaboration, $N_{\text{eff}} = 3.15 \pm 0.23$ [8]. In order for the experimental bound to be satisfied, we must require $T_{\nu R} \ll T_{\nu L}$, i.e. the RH neutrinos must decouple from the thermal bath well before Big Bang Nucleosynthesis. We can estimate $T_{\nu R}$ imposing total entropy conservation, $g_{*S}(T) a^3 T^3 = \text{const.}$ We get

$$\left(\frac{T_{\nu R}}{T_\gamma} \right)^3 = \frac{172}{11(4g_{*S}(T_{\nu R,d}) - 21)}, \quad (\text{A.2})$$

with $g_{*S}(T_{\nu R,d})$ the number of relativistic degrees of freedom (in entropy) at the temperature at which the RH neutrinos decouple from the thermal bath. Following the thermal evolution of the universe backwards in time, and adding the RH neutrinos to the SM relativistic degrees of freedom, we have

$$\begin{aligned} m_\mu < T_{\nu R,d} < m_\pi & & g_{*S} &= 39/2, \\ m_\pi < T_{\nu R,d} < T_{\text{quark-hadron}} & & g_{*S} &= 45/2, \\ T_{\text{quark-hadron}} < T_{\nu R,d} < m_c & & g_{*S} &= 67. \end{aligned} \quad (\text{A.3})$$

Using this result in eq. (A.1), we find $T_{\nu R,d} > T_{\text{quark-hadron}} \sim 300$ MeV. The RH neutrinos decoupling temperature can be estimated using eq. (2.3) and comparing with $T_{\nu L,d} \simeq 1$ MeV:

$$\left(\frac{T_{\nu R,d}}{T_{\nu L,d}} \right)^3 \simeq \frac{1}{\rho^2 |\langle m_{\alpha\beta} \rangle|^2 |\langle m_{\rho\sigma} \rangle|^2} \gtrsim \left(\frac{300 \text{ MeV}}{1 \text{ MeV}} \right)^3, \quad (\text{A.4})$$

which can be used to extract an upper bound on ρ . Scanning over the neutrino parameters at 2σ , we find $\rho \lesssim 300 \text{ eV}^{-2}$, which is weaker than the bounds coming from flavor physics we have presented.

Open Access. This article is distributed under the terms of the Creative Commons Attribution License ([CC-BY 4.0](https://creativecommons.org/licenses/by/4.0/)), which permits any use, distribution and reproduction in any medium, provided the original author(s) and source are credited.

References

- [1] P. Minkowski, $\mu \rightarrow e\gamma$ at a rate of one out of 10^9 muon decays?, *Phys. Lett. B* **67** (1977) 421 [[INSPIRE](#)].
- [2] T. Yanagida, *Horizontal symmetry and masses of neutrinos*, in *Proceedings of the Workshop on Unified Theory and Baryon Number of the Universe*, O. Sawada and A. Sugamoto eds., KEK, Tsukuba Japan (1979), pg. 95 [[INSPIRE](#)].
- [3] P. Ramond, *The family group in grand unified theories*, invited talk given at conference C79-02-25, February 1979, pg. 265 [[CALT-68-709](#)] [[hep-ph/9809459](#)] [[INSPIRE](#)].
- [4] M. Gell-Mann, P. Ramond and R. Slansky, *Complex spinors and unified theories*, in *Supergravity*, P. van Nieuwenhuizen and D. Freedman eds., North Holland, Amsterdam The Netherlands (1979) [*Conf. Proc. C* **790927** (1979) 315] [[PRINT-80-0576](#)] [[arXiv:1306.4669](#)] [[INSPIRE](#)].
- [5] S. Weinberg, *Baryon and lepton nonconserving processes*, *Phys. Rev. Lett.* **43** (1979) 1566 [[INSPIRE](#)].
- [6] M. Fukugita and T. Yanagida, *Baryogenesis without grand unification*, *Phys. Lett. B* **174** (1986) 45 [[INSPIRE](#)].
- [7] K. Dick, M. Lindner, M. Ratz and D. Wright, *Leptogenesis with Dirac neutrinos*, *Phys. Rev. Lett.* **84** (2000) 4039 [[hep-ph/9907562](#)] [[INSPIRE](#)].
- [8] PLANCK collaboration, P.A.R. Ade et al., *Planck 2015 results. XIII. Cosmological parameters*, [arXiv:1502.01589](#) [[INSPIRE](#)].
- [9] S. Gabriel and S. Nandi, *A new two Higgs doublet model*, *Phys. Lett. B* **655** (2007) 141 [[hep-ph/0610253](#)] [[INSPIRE](#)].
- [10] S.M. Davidson and H.E. Logan, *Dirac neutrinos from a second Higgs doublet*, *Phys. Rev. D* **80** (2009) 095008 [[arXiv:0906.3335](#)] [[INSPIRE](#)].
- [11] P.A.N. Machado, Y.F. Perez, O. Sumensari, Z. Tabrizi and R.Z. Funchal, *On the viability of minimal neutrinophilic two-Higgs-doublet models*, [arXiv:1507.07550](#) [[INSPIRE](#)].
- [12] DAYA BAY collaboration, F.P. An et al., *New measurement of antineutrino oscillation with the full detector configuration at Daya Bay*, *Phys. Rev. Lett.* **115** (2015) 111802 [[arXiv:1505.03456](#)] [[INSPIRE](#)].
- [13] DOUBLE CHOOZ collaboration, Y. Abe et al., *Improved measurements of the neutrino mixing angle θ_{13} with the Double CHOOZ detector*, *JHEP* **10** (2014) 086 [*Erratum ibid.* **02** (2015) 074] [[arXiv:1406.7763](#)] [[INSPIRE](#)].
- [14] S. Zhou, *Comment on astrophysical consequences of a neutrinophilic 2HDM*, *Phys. Rev. D* **84** (2011) 038701 [[arXiv:1106.3880](#)] [[INSPIRE](#)].
- [15] BABAR collaboration, J.P. Lees et al., *Evidence for an excess of $\bar{B} \rightarrow D^{(*)}\tau^-\bar{\nu}_\tau$ decays*, *Phys. Rev. Lett.* **109** (2012) 101802 [[arXiv:1205.5442](#)] [[INSPIRE](#)].

- [16] O. Deschamps, S. Descotes-Genon, S. Monteil, V. Niess, S. T’Jampens and V. Tisserand, *The two Higgs doublet of type II facing flavour physics data*, *Phys. Rev. D* **82** (2010) 073012 [[arXiv:0907.5135](#)] [[INSPIRE](#)].
- [17] A. Crivellin, A. Kokulu and C. Greub, *Flavor-phenomenology of two-Higgs-doublet models with generic Yukawa structure*, *Phys. Rev. D* **87** (2013) 094031 [[arXiv:1303.5877](#)] [[INSPIRE](#)].
- [18] M.C. Gonzalez-Garcia, M. Maltoni and T. Schwetz, *Updated fit to three neutrino mixing: status of leptonic CP-violation*, *JHEP* **11** (2014) 052 [[arXiv:1409.5439](#)] [[INSPIRE](#)].
- [19] E. Giusarma, R. de Putter, S. Ho and O. Mena, *Constraints on neutrino masses from Planck and galaxy clustering data*, *Phys. Rev. D* **88** (2013) 063515 [[arXiv:1306.5544](#)] [[INSPIRE](#)].
- [20] J.M. Roney, *Tau physics prospects at SuperB*, *Nucl. Phys. Proc. Suppl.* **169** (2007) 379 [[INSPIRE](#)].
- [21] T. Fukuyama and K. Tsumura, *Detecting Majorana nature of neutrinos in muon decay*, [arXiv:0809.5221](#) [[INSPIRE](#)].
- [22] PARTICLE DATA GROUP collaboration, K.A. Olive et al., *Review of particle physics*, *Chin. Phys. C* **38** (2014) 090001 [[INSPIRE](#)].
- [23] HEAVY FLAVOR AVERAGING GROUP (HFAG) collaboration, Y. Amhis et al., *Averages of b-hadron, c-hadron and τ -lepton properties as of summer 2014*, [arXiv:1412.7515](#) [[INSPIRE](#)].
- [24] BABAR collaboration, B. Aubert et al., *Measurements of charged current lepton universality and $|V_{us}|$ using tau lepton decays to $e^-\bar{\nu}_e\nu_\tau$, $\mu\bar{\nu}_\mu\nu_\tau$, $\pi^-\nu_\tau$ and $K^-\nu_\tau$* , *Phys. Rev. Lett.* **105** (2010) 051602 [[arXiv:0912.0242](#)] [[INSPIRE](#)].
- [25] MEG collaboration, J. Adam et al., *New constraint on the existence of the $\mu^+ \rightarrow e^+\gamma$ decay*, *Phys. Rev. Lett.* **110** (2013) 201801 [[arXiv:1303.0754](#)] [[INSPIRE](#)].
- [26] BABAR collaboration, B. Aubert et al., *Searches for lepton flavor violation in the decays $\tau^\pm \rightarrow e^\pm\gamma$ and $\tau^\pm \rightarrow \mu^\pm\gamma$* , *Phys. Rev. Lett.* **104** (2010) 021802 [[arXiv:0908.2381](#)] [[INSPIRE](#)].
- [27] A.M. Baldini et al., *MEG upgrade proposal*, [arXiv:1301.7225](#) [[INSPIRE](#)].
- [28] MEG II collaboration, T. Iwamoto, *The LXe calorimeter and the pixelated timing counter in the MEG II experiment*, *2014 JINST* **9** C09037 [[INSPIRE](#)].
- [29] T. Toma and A. Vicente, *Lepton flavor violation in the scotogenic model*, *JHEP* **01** (2014) 160 [[arXiv:1312.2840](#)] [[INSPIRE](#)].
- [30] SINDRUM collaboration, U. Bellgardt et al., *Search for the decay $\mu^+ \rightarrow e^+e^+e^-$* , *Nucl. Phys. B* **299** (1988) 1 [[INSPIRE](#)].
- [31] A. Blondel et al., *Research proposal for an experiment to search for the decay $\mu \rightarrow eee$* , [arXiv:1301.6113](#) [[INSPIRE](#)].
- [32] E. Arganda, M.J. Herrero and A.M. Teixeira, *μ -e conversion in nuclei within the CMSSM seesaw: universality versus non-universality*, *JHEP* **10** (2007) 104 [[arXiv:0707.2955](#)] [[INSPIRE](#)].
- [33] Y. Kuno and Y. Okada, *Muon decay and physics beyond the standard model*, *Rev. Mod. Phys.* **73** (2001) 151 [[hep-ph/9909265](#)] [[INSPIRE](#)].
- [34] COMET collaboration, Y. Kuno, *A search for muon-to-electron conversion at J-PARC: the COMET experiment*, *Prog. Theor. Exp. Phys.* **2013** (2013) 022C01 [[INSPIRE](#)].

- [35] SINDRUM II collaboration, C. Dohmen et al., *Test of lepton flavor conservation in $\mu \rightarrow e$ conversion on titanium*, *Phys. Lett. B* **317** (1993) 631 [INSPIRE].
- [36] A. Alekou et al., *Accelerator system for the PRISM based muon to electron conversion experiment*, [arXiv:1310.0804](#) [INSPIRE].
- [37] SINDRUM II collaboration, W.H. Bertl et al., *A search for muon to electron conversion in muonic gold*, *Eur. Phys. J. C* **47** (2006) 337 [INSPIRE].
- [38] A. Abada, V. De Romeri, S. Monteil, J. Orloff and A.M. Teixeira, *Indirect searches for sterile neutrinos at a high-luminosity Z-factory*, *JHEP* **04** (2015) 051 [[arXiv:1412.6322](#)] [INSPIRE].
- [39] ATLAS collaboration, *Search for the lepton flavor violating decay $Z \rightarrow e\mu$ in pp collisions at $\sqrt{s} = 8$ TeV with the ATLAS detector*, *Phys. Rev. D* **90** (2014) 072010 [[arXiv:1408.5774](#)] [INSPIRE].
- [40] DELPHI collaboration, P. Abreu et al., *Search for lepton flavor number violating Z^0 decays*, *Z. Phys. C* **73** (1997) 243 [INSPIRE].
- [41] CMS collaboration, *Search for lepton-flavour-violating decays of the Higgs boson*, *Phys. Lett. B* **749** (2015) 337 [[arXiv:1502.07400](#)] [INSPIRE].
- [42] LEP, DELPHI, OPAL, ALEPH and L3 collaborations, G. Abbiendi et al., *Search for charged Higgs bosons: combined results using LEP data*, *Eur. Phys. J. C* **73** (2013) 2463 [[arXiv:1301.6065](#)] [INSPIRE].